^{27}Al{^{1}H} Cross Polarization Triple-Quantum Magic Angle Spinning NMR

C. Fernandez,*,† L. Delevoye,† J.-P. Amoureux,† D. P. Lang,‡ and M. Pruski‡

Contribution from the Laboratoire de Dynamique et Structure des Matériaux Moléculaires, CNRS URA 801, 59655 Villeneuve d'Ascq Cedex, France, and Ames Laboratory, 230 Spedding Hall, Ames, Iowa 50011

Received December 27, 1996. Revised Manuscript Received April 11, 1997[⊗]

Abstract: An experiment is described that produces multiple-quantum magic angle spinning (MQMAS) NMR spectrum of ^{27}Al via ^{1}H cross polarization (CP). An application of this new technique to the study of a fully hydrated $AlPO_4$-11 aluminophosphate is presented. It is shown that a combination of MQMAS and CPMQMAS provides new insight into the structure of this sample. While MQMAS alone can be used to obtain high-resolution spectra and quantitative information on the distribution of Al sites, CPMQMAS allows one to establish the positions of water molecules within the $AlPO_4$-11 framework.

Introduction

Spectral resolution for solid state NMR of quadrupolar nuclei has recently been enhanced with the development of the multiple-quantum magic angle spinning (MQMAS) method by L. Frydman and J. S. Harwood.[1] Several improvements have been made to this technique during the past year. These include optimization of the conditions for excitation of multiple-quantum (MQ) coherences,[2,3] the development of different methods to produce pure-absorption spectra,[4−8] and the elimination of spinning sidebands in the MQ dimension using synchronization of the dwell time with the rotor period.[9] The sensitivity of the triple-quantum (3Q) MQMAS technique was proven to be excellent for many applications dealing with several important quadrupolar nuclei, e.g., ^{23}Na,[5,6,8,10] ^{11}B,[11] ^{87}Rb,[4,5] and ^{27}Al.[5,6,12−14] For ^{27}Al, quintuple-quantum (5Q) MQMAS spectra have also been obtained,[15−18] leading to significant improvement in resolution. Compared to other high-resolution techniques such as double-rotation (DOR) and dynamic angle spinning (DAS),[19−21] which suffer from mechanical limitations, the MQMAS method is relatively easy to use.

The basic MQMAS technique can be further enhanced by incorporating it with cross polarization (CP).[22,23] The authors have shown recently that such a CPMQMAS experiment is possible between ^{19}F and ^{27}Al in a fluorinated triclinic chabazite-like $AlPO_4$ aluminophosphate.[24] A clear discrimination between the fluorinated and nonfluorinated Al sites was achieved, which demonstrated the utility of CPMQMAS for spectral editing. In this paper, we show the first CPMQMAS experiment between ^{1}H and ^{27}Al spins and provide a detailed description of the experimental method used. Furthermore, we show that MQMAS can be used to obtain quantitative determination of the distribution of aluminium sites in a sample. The experiments were performed using a fully rehydrated form of $AlPO_4$-11 aluminophosphate,[25] and their results will be compared with those obtained earlier using MAS,[26] DOR,[26−28] and CPDOR[29,30] techniques.

High-Resolution MQMAS Experiment

The MQMAS method is a two-dimensional (2D) experiment capable of averaging the second-order quadrupolar interaction

* Correspondence should be addressed to Christian.Fernandez@univ-lille1.fr (e-mail).
† CNRS URA 801.
‡ Ames Laboratory.
⊗ Abstract published in *Advance ACS Abstracts,* July 1, 1997.

(1) Frydman, L.; Harwood, J. S. *J. Am. Chem. Soc.* **1995**, *117*, 5367.
(2) Amoureux, J.-P.; Fernandez, C.; Frydman, L. *Chem. Phys. Lett.* **1996,** *259*, 347.
(3) Wu, G.; Rovnyank, D.; Sun, B.; Griffin, R. G. *Chem. Phys. Lett.* **1995**, *249*, 210.
(4) Fernandez, C.; Amoureux, J.-P. *Solid State NMR* **1996**, *5*, 315.
(5) Massiot, D.; Touzo, B.; Trumeau, D.; Coutures, J. P.; Virlet, J.; Florian P.; Grandinetti, P. J. *Solid State NMR* **1996**, *6*, 73.
(6) Medek, A.; Harwood, J. S.; Frydman, L. *J. Am. Chem. Soc.* **1995**, *247*, 12779.
(7) Amoureux, J.-P.; Fernandez, C.; Steuernagel, S. *J. Magn. Reson.* **1996**, *A123*, 116
(8) Brown, S. P.; Heyes S. J.; Winperis, S. *J. Magn. Reson.* **1996**, *A119*,-280.
(9) Massiot, D. *J. Magn. Reson.* **1996**, *A122*, 240.
(10) Massiot, D.; Conanec, R.; Feldmann, W.; Marchand, R.; Laurent, Y. *Inorg. Chem.* **1996**, *35*, 4957.
(11) Hwang, S. J.; Fernandez, C.; Amoureux, J.-P.; Cho, J.; Martin, S. W.; Pruski, M. *Solid State NMR* **1997**, *8*, 109.
(12) Fernandez, C.; Amoureux, J.-P.; Chezeau, J. M.; Delmotte, L.; Kessler, H. *Microporous Mater.* **1996**, *6*, 331.
(13) Rocha, J.; Esculas, A.; Fernandez, C.; Amoureux, J.-P. *J. Phys. Chem.* **1996**, *100*, 17889.
(14) Baltisberger, J. H.; Xu, Z.; Stebbins, J. F.; Wang S. H.; Pines, A. *J. Am. Chem. Soc.* **1996**, *118*, 7209.
(15) Fernandez, C.; Amoureux, J.-P. *Chem. Phys. Lett.* **1995**, *242*, 449.
(16) Fernandez, C.; Amoureux, J.-P.; Delmotte, L.; Kessler, H. *Microporous Mater.* **1996**, *6*, 125.
(17) Rocha, J.; Lin, Z.; Fernandez, C.; Amoureux, J.-P. *Chem. Commun.* **1996**, 2513
(18) Sarv, P.; Fernandez, C.; Amoureux, J.-P.; Keskinen, K. *J. Phys. Chem.* **1996**, 100, 19223.
(19) Llor A.; Virlet, J. *Chem. Phys. Lett.* **1988**, *152*, 248.
(20) Samoson, A.; Lippmaa E.; Pines, A. *Mol. Phys.* **1988**, *65*, 1013.
(21) Mueller, K. T.; Sun, B. Q.; Chingas, G. C.; Zwanziger, J. W.; Terao T.; Pines, A. *J. Magn. Reson.* **1990**, *86*, 470.
(22) Hartmann S. R.; Hahn, E. L. *Phys. Rev.* **1964**, *128*, 2042.
(23) Pines, A.; Gibby M. G.; Waugh, J. S. *J. Chem. Phys.* **1973**, *59*, 569.
(24) Pruski, M.; Lang, D. P.; Fernandez C.; Amoureux, J.-P. *Solid State NMR* **1997**, *7*, 327.
(25) Khouzami, R.; Coudurier, G.; Lefebvre, F.; Vedrine J. C.; Mentzen, B. *Zeolites* **1990**, *10*, 183.
(26) Barrie, P. J.; Smith M. E.; Klinowski, J. *Chem. Phys. Lett.* **1991**, *180*, 6.
(27) Peeters, M. P. J.; De Haan, J. W.; Van de Ven, L. J. M.; Van Hooff, J. H. C. *J. Phys. Chem.* **1993**, *97*, 5363.
(28) Peeters, M. P. J.; Van de Ven, L. J. M.; De Haan, J. W.; Van Hooff, J. H. C. *J. Phys. Chem.* **1993**, *97*, 8254.
(29) Wu, Y.; Lewis, D.; Frye, J. S.; Palmer A. R.; Wind, R. A. *J. Magn. Reson.* **1993**, *100*, 425.
(30) Sun, W.; Stephen, J. T.; Potter L. D.; Wu, Y. *J. Magn. Reson.* **1995**, *116*, 181.

S0002-7863(96)04440-X CCC: $14.00

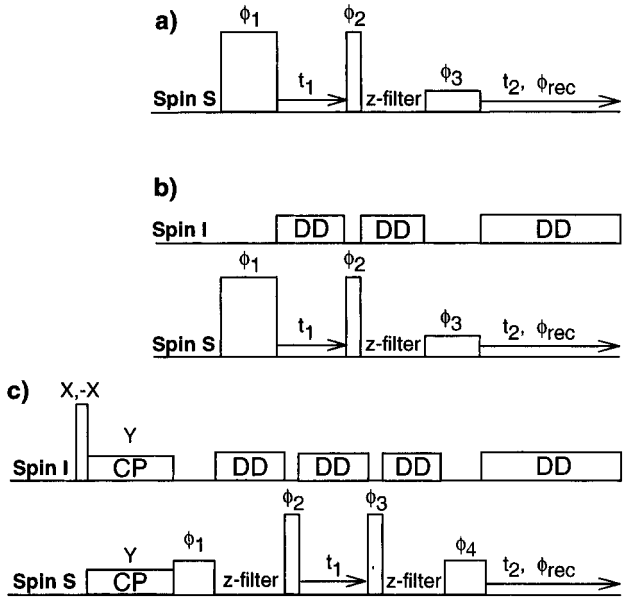

Figure 1. Schematic diagram of (a) MQMAS with *z*-filter, (b) DDMQMAS, and (c) CPMQMAS pulse sequences.

of half-integer nuclear spins ($S > {}^1/_2$).[1] Briefly, in the fast MAS spinning speed limit, the line shape of the MQ powder spectrum of quadrupolar nuclei is governed by the expression[31]

$$\delta(\alpha,\beta) = \delta_{CS} + \delta_{QIS}(S,p,C_Q,\eta) + A_4(S,p)\,B_4(\alpha,\beta,C_Q,\eta) \tag{1}$$

where $\delta(\alpha,\beta)$ represents the resonance shift (in ppm), as a function of the polar angles α and β describing the orientation of the rotor axis with respect to the quadrupolar tensor, δ_{CS} is the isotropic chemical shift, δ_{QIS} is the quadrupolar induced shift, p is the order of the MQ coherence corresponding to the nondiagonal elements ($+p/2$, $-p/2$) of the density matrix, and C_Q and η are the quadrupolar coupling constant and asymmetry parameter, respectively. A_4 and B_4 terms were given explicitly in ref 31. The ppm scale is defined with respect to the apparent Larmor frequency $-p\nu_0$. The MQMAS experiment is designed to refocus the anisotropy of the quadrupolar interaction, which is represented by the third term in eq 1. This refocusing is achieved by correlating the evolution of the MQ coherences ($\pm p/2$, $\mp p/2$) during t_1 and the observable single-quantum central transition coherence ($-{}^1/_2$,$+{}^1/_2$) during t_2. Using the pulse sequence shown in Figure 1a, an echo is observed at

$$t_{2e} = |A_4(S,p)/A_4(S,-1)|t_1 = Rt_1 \tag{2}$$

Echoes are generated in a two-dimensional way by incrementing t_1. A 2D Fourier transformation with respect to t_1 and t_2 leads to the MQMAS spectrum. Among the different procedures used to obtain pure-absorption 2D spectra,[4−8] we found the z-filter method[7] to be the most advantageous (see below).

The typical MQMAS spectra of polycrystalline samples consist of narrow two-dimensional ridges that are extended along the direction given by the *R/p* ratio.[15] An orthogonal projection of this 2D spectrum onto the F_2 dimension resembles the conventional MAS spectrum, although with pQ-filtered intensities. The F_1 projection corresponds to the *p*-quantum spectrum. The analysis of the MQMAS spectra is assisted by applying a shearing transformation that places the anisotropic direction perpendicular to the isotropic axis, F_1^{ISO}. Such a transformation can be performed either in the frequency domain or in the time domain using the phase shift theorem.[5,32]

The center of gravity of a powder spectrum of quadrupolar nuclei is not observed at the isotropic chemical shift δ_{CS}, but is displaced from it by δ_{QIS} in the F_2 dimension and by δ_{QIS}^{ISO} in the F_1^{ISO} dimension of the sheared 2D spectrum. These quadrupolar induced shifts are given in parts per million by the following expressions:

$$\delta_{QIS}(S,C_Q,\eta) = -\frac{3}{10}[4S(S+1)-3]\left\{\frac{SOQE}{4S(2S-1)\nu_0}\right\}^2 \times 10^6 \tag{3}$$

and

$$\delta_{QIS}^{ISO}(S,C_Q,\eta) = -\frac{10}{17}\delta_{QIS}(S,C_Q,\eta) \tag{4}$$

where $SOQE = C_Q(1 + \eta^2/3)^{1/2}$ defines the second-order quadrupolar effect parameter.

Thus, the center of gravity of different species with the same δ_{CS} but different SOQE parameters are located along the so-called QIS direction with a slope $\xi = -10/17$. Similarly, species experiencing the same quadrupolar interactions, but different isotropic chemical shifts, will be located along a direction parallel to the CS axis with a slope of 1 (Figure 2a).

Note that the slopes of the CS and QIS axes do not depend on the coherence *p* chosen to perform the MQMAS experiment. Consequently, the 3QMAS and 5QMAS spectra of ^{27}Al should be similar in the fast spinning speed limit. However, experimental resolution between different sites can be enhanced in 5QMAS.[15−18]

CPMQMAS Experiment

The main difference between MQMAS and CPMQMAS experiments is in the preparation period. In both techniques, the preparation pulses are used to create and maximize the $\rho_{+p/2,-p/2}$ and $\rho_{-p/2,+p/2}$ elements of the density matrix of the observed spins *S*. To use the CPMQMAS experiment for spectral editing, it is essential to achieve efficient coherence transfer that proceeds via the *I* spins and to eliminate the effect of direct *S* polarization. While a direct excitation of the multiple-quantum coherences can be conceivably achieved via cross polarization,[33,34] in this work, we chose a more approachable coherence transfer scheme ($0 \rightarrow \pm 1 \rightarrow 0 \rightarrow \pm 3 \rightarrow 0 \rightarrow -1$). The implementation of this scheme becomes relatively easy with the use of a pair of *z*-filters.[7] Below, we describe the experimental setup of the CPMQMAS experiment, which relies upon maximizing the transfer of *S* magnetization obtained using $I \rightarrow S$ cross polarization process through the selected coherence pathways.

It is well-known that cross polarization of quadrupolar spins is difficult, even with conventional MAS. The major difficulty, which was systematically studied by A. Vega,[33,34] is in maintaining spin locking of the central transition coherence under MAS. The spin locking efficiency can be expressed in terms of the parameter

$$\alpha = \nu_{1S}^2/\nu_Q\nu_r \tag{5}$$

where ν_{1S} is the amplitude of the radio frequency (rf) field for the *S* nuclei being cross polarized, $\nu_Q = 3C_Q/2S(2S-1)$ is the quadrupolar frequency, and ν_r is the sample spinning frequency.

(31) Amoureux, J.-P. *Solid State NMR* **1993**, *2*, 83.

(32) Ernst, R. R.; Bodenhausen G.; Wokaun A. *Principles of Nuclear Magnetic Resonance in One and Two Dimensions*; Clarendon Press: Oxford, U.K., 1987.

(33) Vega, A. J. *J. Magn. Reson.* **1992**, *96*, 50.

(34) Vega, A. J. *Solid State NMR* **1992**, *1*, 17.

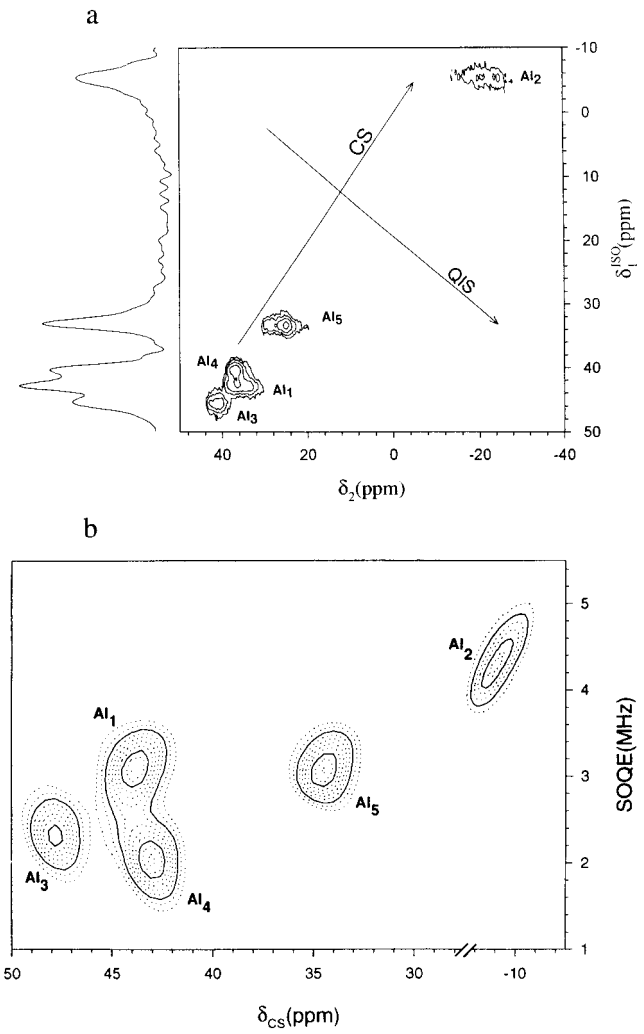

Figure 2. (a) 3QMAS spectrum of the calcined and fully rehydrated $AlPO_4$-11: Rf field amplitude $\nu_{1S} = 300$ kHz, spinning speed $\nu_r = 14$ kHz, dwell time in t_1 set to $1/\nu_r$, number of accumulations per row of data: 24, delay for T_1 relaxation: 500 ms, number of t_1 increments: 128, approximate acquisition time: 30 min. The resonances are labeled by following the assignment given by Peeters et al.[27] (b) Canonical representation obtained from inversion of the 3QMAS spectrum.

Vega showed that the spin locking efficiency can be preserved under adiabatic ($\alpha \gg 1$) or rapid passage conditions ($\alpha \ll 1$) but becomes nearly impossible in the intermediate regime ($\alpha \approx 0.4$). Later work by Sun et al.[30] showed that the most efficient locking is achieved when $\alpha \ll 1$, which is satisfied using a high spinning speed and a weak rf field during the CP transfer. Furthermore, care must be taken to avoid the resonance condition $\nu_r = k\nu_{1S}$.[30]

The first part of the CPMQMAS experiment, referred to as the CP in Figure 1c, relies upon optimization of the CP conditions to maximize the ($\pm 1/2, \mp 1/2$) elements of the density matrix of the *S* spins in the same manner as in conventional CPMAS. These coherences will, however, include contributions from the direct polarization of the *S* spins; thus, it is important to apply a 180° phase alternation to the *I* spin excitation pulse.[34] For quadrupolar nuclei, a highly selective excitation of the ($\pm 1/2, \mp 1/2$) coherences can be obtained using the Hartmann−Hahn matching condition

$$\nu_{1I} = (S + {}^1/_2)\nu_{1S} \pm n\nu_r \qquad (6)$$

where ν_{1I} is the strength of the rf field applied to the *I* spins.

The second part of the sequence, the multiple-quantum evolution and excitation period, is designed to transfer the single-quantum coherences ($\pm 1/2, \mp 1/2$) created via CP to 3Q coherences ($\pm 3/2, \mp 3/2$) with the highest possible efficiency. This can be efficiently achieved using a *z*-filter followed by a strong rf pulse (see Figure 1c). The *z*-filter consists of a "soft" (selective) 90° pulse which, in this case, stores the CP magnetization along the direction of the magnetic field $\vec{B}_0$. After a suitable delay introduced in order to dephase the undesired components of the density matrix, the ($\pm 3/2, \mp 3/2$) coherences are produced in the standard way by a strong rf pulse which is followed by the evolution period.

The last part of the sequence, referred to as the observation period, transfers the ($\pm 3/2, \mp 3/2$) coherences to an observable single-quantum ($-{}^1/_2, +{}^1/_2$) coherence. Again, a *z*-filter scheme is used to symmetrize the coherence transfer pathway, composed of a strong rf pulse that transfers the triple-quantum coherences to zero-quantum coherences followed by a selective 90° pulse to create observable signal.[7] The phase cycling used in this experiment consisted of 24 phases, as shown in Table 1. Two-dimensional spectra were acquired using the hypercomplex method to obtain phase separation. Other phase cycling methods, including a 48-phase scheme (with two-phase cycling of ϕ_1) and a 96-phase scheme (CYCLOPS-based), did not result in further improvement of the observed spectra. Since the optimization of the CP process and of the multiple-quantum coherence transfer can be done independently, we found the setup of the CPMQMAS experiment to be relatively straightforward. We note, however, that the spin dynamics of the cross polarization process is very complex. In particular, the experiment is sensitive to the the resonance offset of both *I* and *S* spins and the spinning speed, especially when very low-rf power is used for cross polarization.

Experimental Section

The ^{27}Al 3QMAS spectra without and with ^{1}H dipolar decoupling (DD) were taken at 9.4 T on a Bruker DSX 400 spectrometer using the pulse sequences depicted in Figure 1, parts a and b, respectively. The spectrometer was equipped with a newly developed, 4 mm MAS probehead capable of producing an rf field of 300 kHz and an MAS speed of 14 kHz. The CPMQMAS experiment (Figure 1c) was performed on a Bruker ASX 400 using a 4 mm CPMAS probehead working with a maximum ν_{1S} rf field of 60 kHz. The Hartmann−Hahn condition was established with an rf field $\nu_{1S} = 5$ kHz, under an MAS speed of 12 kHz. Proton decoupling during the evolution and acquisition times was performed using $\nu_{1I} = 80$ kHz.

The $AlPO_4$-11 sample was provided by the Laboratoire des Matériaux Minéraux (ENSCM, Mulhouse, France). It was calcined and fully rehydrated prior to the NMR experiments.

Results and Discussion

The result of a standard 3QMAS experiment performed with the hydrated $AlPO_4$-11 sample is shown in Figure 2a. Five distinct aluminum resonances are observed in the isotropic projection of the two-dimensional spectrum, which is similar to the results obtained previously using DOR.[27,28] It is known that $AlPO_4$-11 has a structure consisting of AlO_4^- and PO_4^+ tetrahedra connected by bridging oxygen atoms to form a one-dimensional, 10-membered ring pore system.[35,36] The dehydrated $AlPO_4$-11 has three distinct crystallographic Al sites with 2:2:1 occurrences, while the fully rehydrated form undergoes changes in symmetry leading to five different crystallographic Al sites[25] of equal population. In general, polar molecules such as water or ammonia can coordinate to a part of the framework aluminum sites in aluminophosphates and change the alumi-

(35) Bennett, J. M.; Richardson, J. W., Jr.; Pluth J. J.; Smith, J. V. *Zeolites* **1987**, *7*, 160.
(36) Richardson, J. W.; Pluth J. J.; Smith, J. V. *Acta Crystallogr*. **1988**, *B44*, 367.

Table 1. Basic Phase-Cycling Scheme Used in the $^1H-^{27}Al$ CP3QMAS Experiment[a]

$\pi/2$	x	x	$-x$	$-x$
CP (I)	y	y	y	y
CP (S)	0°	0°	0°	0°
ϕ_1	90°	90°	90°	90°
ϕ_2	0°	0°	0°	0°
ϕ_3	0°, 60°, 120°, 180°, 240°, 300°	0°, 60°, 120°, 180°, 240°, 300°	0°, 60°, 120°, 180°, 240°, 300°	0°, 60°, 120°, 180°, 240°, 300°
ϕ_4	0°	180°	0°	180°
ϕ_{rec}	0°, 180°, 0°, 180°, 0°, 180°	0°, 180°, 0°, 180°, 0°, 180°	0°, 180°, 0°, 180°, 0°, 180°	0°, 180°, 0°, 180°, 0°, 180°

[a] The phase notation is consistent with the scheme of Figure 1c.

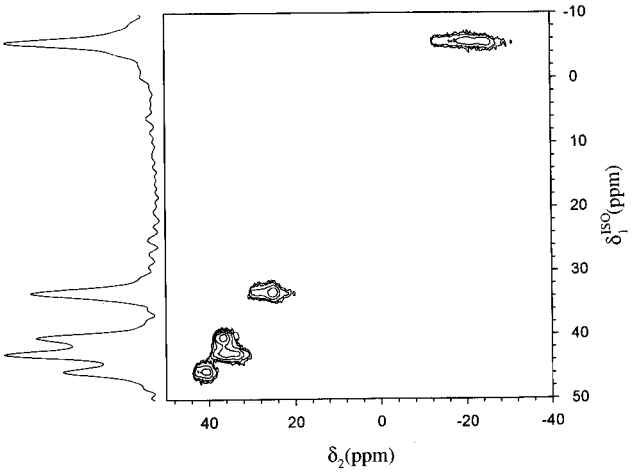

Figure 3. ^1H DD3QMAS spectrum of the calcined and fully rehydrated $AlPO_4$-11. Experimental conditions are identical to those of Figure 2.

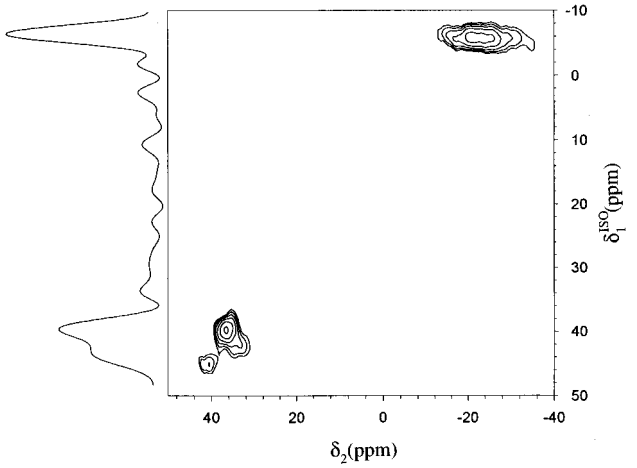

Figure 4. $^1H-^{27}Al$ CP3QMAS spectrum of the calcined and fully rehydrated $AlPO_4$-11: Rf field amplitude during the 500 μs CP contact time $\nu_{1S} = 5$ kHz, rf field amplitude during "soft" pulses $\nu_{1S} = 10$ kHz, rf field amplitude during "hard" pulses $\nu_{1S} = 60$ kHz, spinning speed $\nu_r = 12$ kHz, dwell time in t_1 set to $1/\nu_r$, number of accumulations per row of data: 1200, delay for T_1 relaxation: 1.5 s, approximate experimental time: 16 h.

num's symmetry from tetrahedral to five- or six-coordinated. The NMR results show that, in $AlPO_4$-11, only four- and six-coordinated species were observed following hydration.[27]

We note here that, for a given rf field, the integrated intensities of the 2D MQMAS resonances strongly depend on the value of the quadrupolar coupling constant and on the crystallite orientation (α,β).[2] Therefore, strong line shape distortions are possible, especially when the rf field is not large compared to the MAS line width. Although the use of high-power MAS probes capable of producing an rf field of up to 300 kHz (such as one designed for this work) can reduce these experimental distortions, reliable spectral information can only be obtained with the aid of numerical methods. One possible strategy relies upon the MQMAS experiment to obtain high-resolution and isotropic chemical shifts and using it for the simulation of one-dimensional, quantitative MAS spectra to obtain quadrupolar parameters and relative intensities.[11] We have recently developed another numerical method that allows quantitative determination of the distributions of δ_{CS} and SOQE parameters directly from the 2D MQMAS spectrum. The strategy utilizes a leapfrog method to compute the evolution of the density matrix under the rf power and spinning conditions used in the experiment.[37] Applying this method to the spectrum of Figure 2a leads to the canonical representation[37−39] displayed in Figure 2b. The relative intensities found using this method are in remarkably good agreement with the expected 1:1:1:1:1 Al site population in $AlPO_4$-11.[25]

The interaction of the water molecules with the aluminophosphate framework can be probed using the 3QMAS experiment with high-power (80 kHz) proton dipolar decoupling (DDMQMAS), according to the sequence shown in Figure 1b. The resulting spectrum (Figure 3) shows that the resonances from the octahedral site Al_2 and the tetrahedral sites Al_1, Al_3, and Al_4 were visibly narrowed in the MQ isotropic dimension. On the other hand, ^1H decoupling has negligible effect on resolution in the anisotropic dimension. This effect is not surprising because the apparent strength of the dipolar interaction in the isotropic dimension of the 3QMAS spectrum is enhanced by a factor of 3 and the resulting broadening cannot be completely removed by MAS at 14 kHz.

The CPMQMAS spectrum of the same sample is shown in Figure 4. Clearly, this technique provides more direct information about the interaction of various aluminum sites with water. It is evident that the Al_2 resonance exhibits the strongest CP intensity, while the Al_5 resonance is essentially absent. These observations are consistent with the previous ^{27}Al DOR NMR and X-ray diffraction data of Peeters et al.[27,28] and the CPDOR results of Wu et al.,[29] which also suggested that the Al_2 and Al_5 sites are the most and the least susceptible to hydration, respectively. Furthermore, the CPMQMAS technique shows that among the remaining tetrahedral sites, Al_4 interacts with water more strongly than Al_1 and Al_3. This observation can be explained if one considers that a water molecule strongly bound to Al_2 by its oxygen atom may also have one of its hydrogens bound with one of the oxygens near Al_4.[28] In this case, the Al_1 and Al_3 atoms are the next nearest neighbors, and thus are also cross polarized, yet less efficiently. In this scenario, the Al_5 is too far away to interact with this water molecule.

When we compare the CPMQMAS experiment with CPDOR,[30] we note that both methods require comparable experimental time. While the tetrahedral Al sites in hydrated $AlPO_4$-11 yielded a slightly better signal-to-noise ratio in a shorter time by the CPDOR (25 000 accumulations versus a total of 38 400 in 2D CPMQMAS), the CPMQMAS method provided a better quality spectrum for the octahedral site. This effect is due to

(37) Fernandez, C.; Delevoye, L.; Amoureux, J. P.; Sarv, P. Manuscript in preparation.
(38) Zwanziger, J. W. *Solid State NMR* **1994**, *3*, 219.
(39) Samoson, A. *J. Magn. Reson.* **1996,** *A121***,** 209.

the presence of several overlapping spinning sidebands in the CPDOR spectrum, which is the common shortcoming of the DOR technique. The CPMQMAS method demands, however, the usage of a very wide range of rf fields which, in turn, requires high-quality linear power amplifiers.

Conclusions

The above results demonstrate that the $^{1}H-^{27}Al$ CPMQMAS method offers a tool for spectral editing of high-resolution MQMAS spectra of ^{27}Al based on the strength of the dipolar coupling with hydrogen. Further extension of this work will include (i) other pairs of nuclei, e.g., $^{31}P-^{27}Al$ CPMQMAS, and (ii) heteronuclear correlation experiments, similar to those performed earlier with MAS and DAS.[40,41]

Acknowledgment. C.F., L.D., and J.-P.A. are grateful to Bruker (S. Steuernagel, F. Engelke, and H. Forster) for technical help and to Dr. L. Delmotte for providing the $AlPO_4$-11 sample. This research was supported, in part, by the U.S. Department of Energy, Office of Basic Energy Sciences, Division of Chemical Sciences, under Contract W-7405-Eng-82.

JA964440V

(40) Fyfe, C. A.; Wong-Moon, K. C.; Huang, Y.; Grondey, H.; Mueller, K. T. *J. Phys. Chem.* **1995**, *99*, 8707.

(41) Jarvie, T. P.; Wenslow R. M.; Mueler, K. T. *J. Am. Chem. Soc*. **1995**, *117*, 570.